Relationship Between Cardiac Isochrones and its Mean Anatomical Position in the Heart: The *CineECG*

Machteld J Boonstra[1], Dana H Brooks[2], Peter Loh[1], Peter M van Dam[1]

[1]UMC Utrecht, Utrecht, the Netherlands
[2]Northeastern University, Boston, United States of America

Abstract

CineECG is a novel approach to ECG analysis relating average cardiac electrical activity to the cardiac anatomy. Since its introduction CineECG has been reported to be reliable for the detection of Brugada Type-1 and conduction disorders, but the relationship between cardiac isochrones and CineECG remains unexplored. To describe this relation, fourteen distinct activation sequences were simulated and resulting ECGs were used to compute the CineECG. The average isochrone position was used as ground truth to compare to CineECG trajectories. The average distance between the CineECG and AIP was 24±3 mm, with significantly better agreement for the terminal QRS segment. Quantitatively, CineECG captures significant features of underlying activation sequences and its direct relation to cardiac anatomy provides additional insight into electrical cardiac pathology.

1.   Introduction

The standard 12-lead ECG is a fundamental clinical tool to provide direct insight into cardiac electrical activity. However, interpretation requires extensive expert training and is subject to considerable inter- and intra-expert variability. Furthermore, interpretation is complicated by the difficulty in linking ECG data to cardiac anatomy and sensitivity of the ECG waveforms to electrode positioning. The vectorcardiogram (VCG) was thought to overcome this problem by representing the magnitude and direction of electrical activity by a rotating vector. However, the VCG is similarly difficult to interpret and still requires a difficult 3D rotation by the interpreter to relate the VCG to the cardiac anatomy.

CineECG is a novel approach for standard 12 lead ECG analysis that directly relates cardiac electrical activity to anatomy [1]. Since its introduction, *CineECG* has been reported to be reliable for the detection of Brugada Type-I and conduction disorders [2,3] and by the presentation of the normal distribution [4] of the *CineECG*, cardiac

pathology can be easily identified. However, the relationship between cardiac isochrones and the *CineECG* has not yet been explored.

2.   Methods

2.1.   *CineECG* methodology

CineECG uses the standard 12-lead ECG to estimate the average position of cardiac activation waveforms within an anatomical 3D heart model. Three inputs are required: 1) 3D anatomical heart/torso model based on CT or MRI imaging, 2) ECG electrode locations, and 3) 12-lead ECG. In **Figure 1**, a schematic representation of the *CineECG* computation is presented.

The *CineECG* computation starts with an initialization step wherein the starting point *in space and time* is located within the ventricular anatomy, which is used to start the bi-directional recursive *CineECG* calculations. For simplicity we only describe the computation going in the forward direction in time; the backward computation is essentially the same.

The starting point is set to the centre of mass of the anatomical 3D heart model and temporally at mid-QRS based at the assumption that at mid-QRS, half of the ventricular mass is activated and thus the average location of the activation wavefront is located near the centre of mass. From the starting point, the average cardiac activation position is propagated through the cardiac anatomy with a two-step procedure. In the first step a modified VCG is computed from the 12-lead ECG at a given time sample using time-dependent lead vectors which points from the previous *CineECG* location to each of the electrodes (**Figure 1**). The time-dependent lead vector is denoted as $\left(\overrightarrow{r_{el}} - \overrightarrow{r_{ref}}(t)\right)$, and where $\overrightarrow{r_{el}}$ is the 3D coordinate of the electrode (el) and $\overrightarrow{r_{ref}}(t)$ is the previous *CineECG* location. Each time-step vector is then normalized. The VCG at time t is calculated as the vector sum of these unit vectors weighted by the unipolar ECG amplitude $ecg_{el}(t)$ and the correction factor α_{el}. this factor is used for differences in distance from the heart to
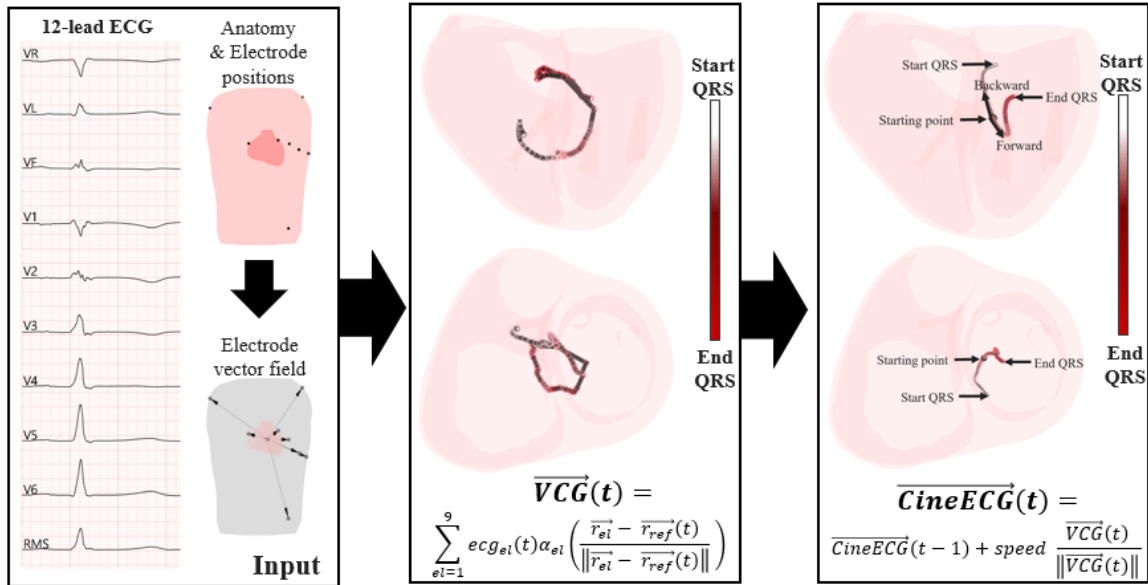
Figure 1 – Schematic representation of the *CineECG* methodology. In the left panel, the inputs for the computation are displayed. Using these inputs, a normalized vectorcardiogram (VCG) is computed (middle panel). Then the current *CineECG* position (right panel) is computed using the direction indicated by the VCG with set speed of 0.7 m/s.

the el[th] electrode (set to 1 for precordial leads and to 2 for unaugmented extremity leads). In the second step, starting from the previous *CineECG* location, the current *CineECG* position is computed by moving along the direction indicated by $\overrightarrow{VCG}(t)$ with a constant propagation speed of 0.7 m/s. The *CineECG* moves from the previous position to the next. The calculation proceeds recursively in this time-step-wise fashion until the entire activation sequence has been localized.

2.2. Simulation of activation sequences

To investigate the relation between cardiac isochrones and *CineECG*, activation sequences were simulated. Therefore, a CT-based volume conductor model of a single subject for the ventricles, blood cavities, lungs and torso (male, 21y) were created. His-Purkinje mediated activation sequences for normal and conduction disorder cases were simulated using the fastest route algorithm with multiple (ranging between 2 and 6) foci located at endocardial locations associated with His-Purkinje mediated activation. Activation sequences were simulated with a constant velocity of 0.85 m/s and an anisotropy ration of 2.5. [5] Fourteen activation sequences were simulated and the *CineECG* and average isochrone position (see 2.2.1) trajectories were computed and compared. These consisted of normal (n=6) and conduction disorder cases (n=8): complete left and right bundle branch blocks (LBBB/RBBB); left anterior/posterior fascicular block (LAFB/LPFB) and incomplete RBBB (iRBBB) were simulated. The boundary element method was used to compute the 12-lead ECG signals of the simulated ventricular activation sequence.

2.2.1. Average Isochrone Position

To compare the *CineECG* to these simulated activation sequences, we developed a new metric to represent the average location of multiple simultaneous activation waves; the average isochrone position (AIP), since the *CineECG* is designed to represent the average location of activation. The AIP is based on the average location per 5ms time interval of the cardiac tissue activated during that interval weighted to local wall thickness. The distance between subsequent AIP locations was no more than 1.5 times the distance between the previous two AIP locations to prevent unphysiologically large jumps between subsequent AIP locations.

2.3. Data analysis

The computed ECG data, the subject specific CT based model and the standard 12-lead ECG precordial electrode positions were used as input for the *CineECG* calculation and trajectories were computed. The AIP trajectories were computed from the simulated activation sequences. The AIP and *CineECG* trajectories were compared per 5ms interval by computing 1) the distance between the locations of the two trajectories, 2) the angle between their directions, 3) the distance of the trajectories to the septal wall and 4) the percentage of the trajectory located in either the left or right ventricular cavity. Average values of the complete, initial (first 25 ms), middle (12 seconds before and after mid-QRS) and terminal (last 25 ms) were determined for the first three metrics.

Data were presented as mean ± standard or range as

Table 1 – Comparison *CineECG* to AIP

	Cases without conduction block (n=6)	Cases with (partial) right conduction block (n=3)	Cases with (partial) left conduction block (n=5)
Number of active foci (n, range)	6	4-5	2-5
Total activation duration (ms)	83±4.1	97±14	96±12
Distance between AIP/*CineECG* complete segment (mm)	24±1	26±3	22±2
Distance between AIP/*CineECG* initial segment (mm)	35±6	31±1	37±8
Distance between AIP/*CineECG* middle segment (mm)	13±3	17±2	11±2
Distance between AIP/*CineECG* terminal segment (mm)	27±1	31±5	20±2
Angle between AIP/*CineECG* complete trajectory (degrees)	76±3	70±5	78±4
Angle between AIP/*CineECG* initial segment (degrees)	113±15	101±10	108±18
Angle between AIP/*CineECG* middle segment (degrees)	66±14	54±10	86±13
Angle between AIP/*CineECG* terminal segment (degrees)	59±5	53±10	44±3

Data are presented by range (number of foci) or as mean ± standard deviation. The initial segment corresponds to the first 25 ms of the denoted trajectory, the terminal segment to the last 25 ms of the trajectory. Distances are calculated between the locations of corresponding time intervals and angles are calculated between the normalized vectors indicating the direction of the trajectory.

appropriate and the data were compared using an (un)paired Student's *t*-test. A 2-sided P-value of <0.05 was considered significant. For the simulation study, differences between the location of the C*ineECG* and AIP per 5 ms time intervals were presented as distances in mm and differences in direction were presented as angles in degrees.

3. Results

Average values of the comparison between *CineECG* and AIP are reported in **Table 1**. The *CineECG* of simulated activation sequences without conduction block stayed closer to the septal wall compared to cases of simulated conduction blocks (**Figure 2**). In all cases, both the terminal *CineECG* and AIP were directed towards the latest activated area. Moreover, as visually inspected, the first 15 ms of the *CineECG* was consistent with the simulated transseptal vector directed towards the side of the septal wall which was activated second. The average

distance between the *CineECG* and AIP trajectories was 24±3 mm and the terminal segment was statistically significantly closer to the AIP than the initial segment (34±6 vs 27±6 mm, p=0.015). The angle between the *CineECG* and AIP direction was 76±5 degrees for the complete trajectory; and similar to the distances, the better aligned than the initial segments (107±15 vs. 51±9 degrees, p<0.001). During the course of the activation, the *CineECG* and AIP became more aligned as reflected in a decrease in directional differences between the AIP and *CineECG* (**Table 1**).

For most of the cases both with and without conduction defects, the *CineECG* trajectory stayed within the left ventricular cavity, whereas the AIP was located more in the right ventricular cavity; for cases with left conduction defects this was true for the initial AIP segment and for cases without conduction defect or with right conduction block for the terminal AIP segment. Both the number and location of used foci affected the shape of the *CineECG*. Decreasing the number of initial sites of activation (**Figure**
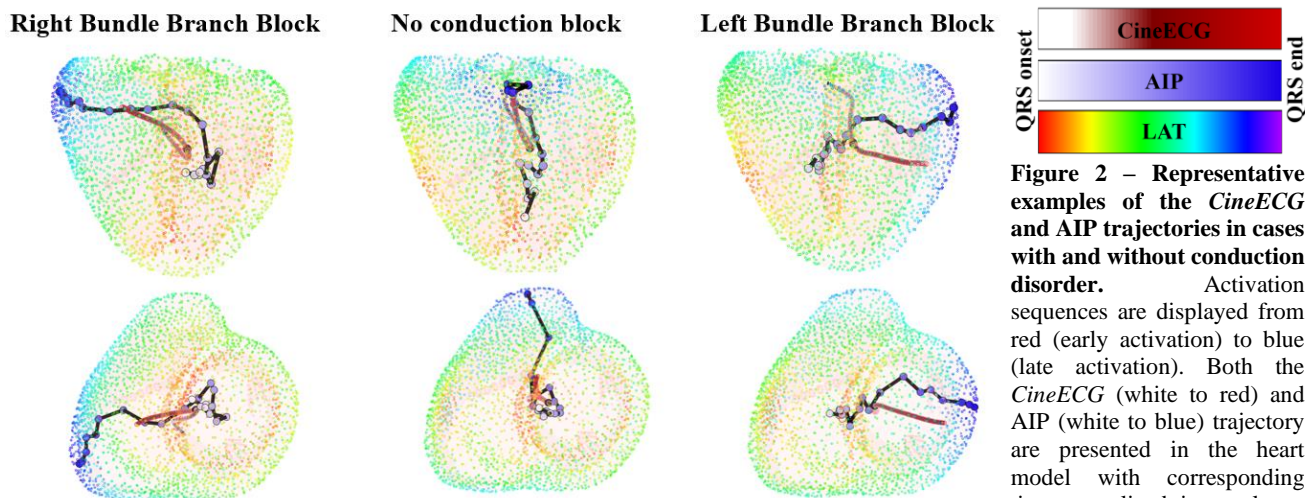
Right Bundle Branch Block **No conduction block** **Left Bundle Branch Block**

Figure 2 – Representative examples of the *CineECG* and AIP trajectories in cases with and without conduction disorder. Activation sequences are displayed from red (early activation) to blue (late activation). Both the *CineECG* (white to red) and AIP (white to blue) trajectory are presented in the heart model with corresponding time normalized time scale.

2, LBBB & RBBB) resulted in less compact *CineECG* in which the initial and terminal parts were located further away from the septum.

4. Discussion

The results presented in this study show that the *CineECG* is able to relate clinically meaningful components of cardiac activation to the cardiac anatomy. The relationship between cardiac activation isochrones and *CineECG* is especially clear in: 1) the terminal segment of the QRS, where *CineECG* moves towards the area of latest activation and 2) the initial segment where the *CineECG* reliably corresponded to the direction of the transseptal vector of the QRS. The overall AIP and *CineECG* trajectories corresponded well visually.

Comparison *CineECG* to AIP

When comparing the AIP to the *CineECG*, the terminal segments of the AIP and *CineECG* aligned better than the initial segments as a higher variation was found in both angle and distance of the initial segments of the AIP and *CineECG* compared to the terminal segments. Whereas the initial segment of the AIP stayed within the center of the heart generally moving in random directions, the *CineECG* had one main direction (**Figure 2**). Variation in the location and number of initial sites of activation affected both the AIP and the *CineECG*. Decreasing the number (without vs with conduction disorder) resulted in a less compact *CineECG* and AIP trajectory, where the initial average direction of activation was less irregular. Furthermore, the location of septal foci in cases without conduction disorder elongated the shape of the *CineECG* and AIP when foci were further apart. It is perhaps not surprising that the greater complexity during the initial segment of cardiac activation resulted in less agreement. In terms of *CineECG*, we note that in the initial segment, when multiple activation wavefronts contribute differently to the recorded ECG signals, information about cardiac activation as measured with ECG is more complex due to compared to the AIP. Factors that influence the resulting ECGs are not only the number of wavefronts but also their geometric relationships (i.e. whether they amplifying or canceling each other), volume conductor effects, and proximity effects. In the terminal QRS segment, wavefronts are collided, thereby decreasing the complexity of the measured ECG. This most likely contributes to the higher disagreement of the AIP and *CineECG* in the initial vs terminal QRS segment.

Study limitations

One limitation of the method is the use of a constant speed of 0.7 m/s to compute the *CineECG*; this assumption is most likely inadequate in the presence of scar/fibrofatty tissue. Additionally, the presence of multiple activation waves can lead to decreased velocity of the "average wavefront" if waves annihilate each other. Further insight into this "average wavefront" velocity can be possibly derived from high density invasive local activation timing maps for the different phases (presence of multiple vs collided waves) of cardiac activation.

Furthermore, an extremely simplified approach for the α_{el}-coefficients is used, fixing them to only two constant values based on limb versus precordial electrode location. However, during the course of the activation sequence, the relationship between the proximity of especially precordial leads and the average activation location may change significantly. Therefore, future work is focused on the incorporation of dynamic α_{el}-coefficient using information from the changing electrode vector field, similar to the VCG computation. Secondly, the comparison between the use of Mason-Likar placed limb electrodes and foot-wrist placed electrodes on the *CineECG* computation should be investigated.

5. Conclusion

With the novel *CineECG*, significant features of underlying activation isochrones are recovered and directly related to cardiac anatomy and the average direction of cardiac activation is imaged from the 12-lead ECG and a simple anatomical model. In summary, *CineECG* directly relates a VCG-like direction to the cardiac anatomy and provides a robust and stable mapping tool which may be broadly useful in the early recognition of cardiac structural abnormalities.

References

[1] P.M. van Dam, "A New Anatomical View on the Vector Cardiogram: the Mean Temporo-spatial Isochrones." *Journal of electrocardiography,* (2017), P732-738.

[2] P.M. van Dam, et al. "Novel CineECG Derived from Standard 12-Lead ECG Enables Right Ventricle Outflow Tract Localization of Electrical Substrate in Patients with Brugada Syndrome." *Circulation: Arrhythmia and Electrophysiology*, (2020), e008524.

[3] M.J. Boonstra, et al. "Novel CineECG Enables Anatomical 3D Localization and Classification of Bundle Branch Blocks." *EP Europace* 23. Supplement_1 (2021), i80-i87.

[4] P.M. van Dam, et al. "The Relation of 12-Lead ECG to the Cardiac Anatomy: The Normal CineECG." *Journal of Electrocardiography*, (2021).

[5] P.M. van Dam, et al. "Non-Invasive Imaging of Cardiac Activation and Recovery." *Annals of Biomedical Engineering*, (2009), P1739-1756.

Address for correspondence: Machteld Boonstra, UMC Utrecht, Department of Cardiology, Heidelberglaan 100, 3508 GA, Utrecht, The Netherlands. machteldboonstra@gmail.com